



Scientific article

UDC 66.092-977.004.942

DOI: 10.52957/27821900\_2023\_01\_142

## MODELLING OF RUBBER THERMAL DEGRADATION KINETICS DURING THE PYROLYSIS OF RUBBER WASTE

M. E. Solovyov<sup>1</sup>, V. F. Kablov<sup>2</sup>, S. L. Baldaev<sup>3</sup>, M. O. Fedorova<sup>3</sup>

Mikhail E. Solovyov, Doctor of Physics and Mathematics, Professor, Viktor F. Kablov, Doctor of Technical Sciences, Professor, Sergey L. Baldaev, Candidate of Technical Sciences, Maria O. Fedorova

<sup>1</sup>Yaroslavl State Technical University, Yaroslavl, Russia, soloviev56@gmail.com

<sup>2</sup>Volzhsky Polytechnic Institute (branch), Volgograd State Technical University, Volzhsky, Russia, kablov@volpi.ru

<sup>3</sup>LCC "Technological Systems of Protective Coatings", Shcherbinka, Moscow, Россия, s.baldaev@tspc.ru, m.fedorova@tspc.ru

---

### Keywords:

worn tyres; rubber waste; pyrolysis; kinetic model, quantum-chemical calculation

**Abstract:** The paper presents the kinetic model of polymer thermodegradation as applied to the process of pyrolysis of worn-out tyres and waste rubber products in an industrial reactor. We calculated the quantum-chemical changes of thermodynamic functions for the probable chemical reactions of mesh elastomer degradation. Solid fraction (carbon black and metal wastes) and vapor-gas mixture separated into three hydrocarbon fractions considered as the reaction products. We use a formal kinetic scheme when describing the kinetics of rubber degradation. It shows the mechanism of the process as a set of radical-chain reactions of polymer degradation. Each hydrocarbon fraction corresponds to a certain set of kinetic constants, the temperature dependences of which are assumed to be Arrhenius. The satisfactory agreement of the obtained calculated thermogravimetric dependences with the experimental data of different authors allowed us to approximate the rubber thermal degradation curves by the curves characterizing the general-purpose rubbers.

---

### For citation:

Solovyev, M.E., Kablov, V.F., Baldaev, S.L. & Fedorova, M.O. (2023) Modelling of rubber thermal degradation kinetics during the pyrolysis of rubber waste, *From Chemistry Towards Technology Step-By-Step*, 4(1), pp. 142-156 [online]. Available at: <http://chemintech.ru/index.php/tor/2023-4-1>

### Introduction

The problem of recycling of worn-out tyres and rubber products, and the waste products of their production has technical-economic and ecological aspects [1]. From the technical and economic point of view, the constant growth of prices for fossil hydrocarbons leads to the necessity of searching efficient ways of their recycling, among which the products based on elastomers are a significant part. From an environmental point of view this type of waste represents a significant hazard due to its low biodegradation rate and the presence of hazardous heavy



metal impurities, mainly zinc. As a result of strict regulatory norms accepted in EU, almost 100% of this kind of waste is recycled [2]. However, the volume of recycling of worn tyres in Russia is significantly low.

There are many ways to recycle worn-out tyres and dismantled rubber products [3]. One of such methods is thermal pyrolysis of this type of waste. It conducted at temperatures above 350 °C without air access [4-6]. The output of the process is the carbon solids fraction which after further purification and crushing can be processed into carbon black, metal wastes and steam-gas mixture of hydrocarbons. They can be separated into fractions and used as fuel. Heavy fractions of hydrocarbons may be used as plasticizers in rubber industry and in production of asphalt concrete. Technologically, the process is organized in a batch or continuous scheme. Catalysts can accelerate the process and increase the yield of light fractions [7-9].

A great number of papers are devoted to the properties of fuels derived from pyrolysis liquid fractions [10-13]. Since the composition of worn tyre rubbers depends on both their manufacturer and size, the fractional composition of pyrolysis-derived fuels can also vary [14]. The use of modern physico-chemical methods of analysis makes it possible to obtain a detailed characterization of these products. Thus, the composition of liquid pyrolysis products of worn-out tyres and municipal polymer waste was analyzed by gas chromatography with mass spectrometric detection (GC-MS) in [15]. Pyrolysis was conducted in a closed reactor at a temperature of 400 °C and a pressure of 50 Pa. It was found that the products obtained included more than three hundred individual compounds. The aromatic compounds (33.5%), followed by naphthenes (28.6%), olefins (19.2%), and paraffins (7.0%) were the greater share of them. The authors of [16] studied the pyrolysis products of waste tyres obtained in a twin-screw extruder. We compared the composition of pyrolysis products when conducting the process without a catalyst and in the presence of CaO as a catalyst. We analyzed the composition of the hydrocarbon fraction using Fourier transform ion cyclotron resonance mass analysis (FT-ICR MS) and  $^1\text{H}$  and  $^{13}\text{C}$  NMR spectroscopy. The hydrocarbon content in the pyrolysis products was 74.9% in the process without catalyst and 78.6% in the presence of CaO. The content of hydrocarbons with one sulphur atom was 14.3% and 13.9%, respectively. The hydrocarbon fraction included aromatic hydrocarbons (26%), tetra-aromatic (13 and 15%), and penta-aromatic (22 and 30%). The authors of [17] studied the pyrolysis process of truck and bus tyresrubber from using zeolite ZSM-5 as a catalyst. A laboratory reactor of closed type with a fixed layer was used as a pyrolysis apparatus. We studied the effect of process temperature in the range of 300-580 °C, the catalyst concentration on the yield of liquid, gaseous hydrocarbon fractions, and their composition and physical properties. It was found that with the increase of process temperature the yield of gaseous pyrolysis fraction increased with the corresponding decrease of liquid fraction. The use of a catalyst allowed us to decrease the pyrolysis temperature and increase the share of the gaseous fraction. The analysis showed that the gaseous fraction, the share of which was 5-30% depending on the process conditions, consists of  $\text{C}_1$ - $\text{C}_4$  hydrocarbons. The analysis of the liquid hydrocarbon fraction by GC-MS showed a wide variety of compounds. The aromatic compounds like benzene, toluene, *o*-xylene, naphthalene and *d*-limonene were the greater share of them.



A kinetic analysis of isoprene and *dl*-limonene formation during pyrolysis of natural rubber based rubbers from worn tyres was attempted in [18]. Thermogravimetry in combination with mass spectroscopy was used. The estimated activation energies of the isoprene and *dl*-limonene formation reactions were 131 and 115 kJ/mol, respectively. The reaction order estimates for these products were 1.2 and 1.1, respectively.

The classic batch pyrolysis process scheme for worn tyres includes [19] their preparation. During it the bead rings can be removed and pre-shredded, loaded into the reactor, and the process conducted at a given temperature. During the process the vapour/gas mixture is extracted from the reactor, the gas fraction is partly consumed to feed the burners for heating the reactor and partly utilized. The liquid fraction enters the condensation unit and separates into fractions. When the process is completed, the reactor is emptied, and the carbon black and metal are separated. Nowadays a variant of structural arrangement of the reactor in the form of a horizontal rotating cylinder is widespread. A variant of such design is given in [20]. In this work we study the pyrolysis products of rubber in this reactor variant.

In order to model and optimize the pyrolysis process of rubber in industrial reactors, first of all, it is necessary to have a system of kinetic reactions equations describing the process of thermodegradation of polymer part of waste. The purpose of this study is the construction of the formal kinetic scheme of the reactions providing the modelling of the kinetics of polymer thermodegradation in the pyrolysis process of the worn-out tyres and rubber waste. This kinetic scheme, on the one hand, should be justified both in terms of the radical-chain mechanism of thermodegradation and the nature of products obtained in the actual production process. On the other hand, this scheme should not be too complex, so that when simulating the operation of a production reactor by solving the coupled problem of heat transfer and chemical kinetics, its implementation does not require excessive computer resources. The following tasks were completed in order to achieve the research purpose: 1) study of pyrolysis products of rubber waste of a real industrial reactor in order to determine their qualitative composition; 2) quantum-chemical simulation of the thermodestruction process of model compounds corresponding by their structure to polymer chain links of rubber waste to determine the individual stages of the reaction scheme.

### Experimental part

In order to construct a formal kinetic scheme, we analyzed the composition of pyrolysis products of worn tyres inside an industrial batch reactor. The reactor shape was cylindrical with a diameter of 2.5 m and length of 9.2 m with a stainless steel wall thickness of 9 mm. It was positioned horizontally on rolling supports with the possibility of slow rotation on them. The reactor was heated at the bottom by three 0.6 MW gas burners and one 0.25 MW liquid burner. The liquid burner was used for the initial heating of the reactor and once the pyrolysis gas fraction started to be released, it was used to feed the gas burners. The automated burner fuel control system ensured that the heating and temperature were maintained at the prescribed levels. The flue gases flowed across the entire surface of the cylinder, thereby achieving uniform



heating. The temperatures of the flue gases at the reactor outlet and of the steam-gas mixture at the reactor outlet were recorded using temperature sensors with a measurement limit of 700 °C and an error of measurement of no more than 0.1 degree. The reactor was loaded with defueled truck and civil car tyres without pre-shredding through a hatch on the front end of the reactor. The same hatch was used to discharge the waste metal wire after the process was completed. The vapour-gas mixture was discharged through an opening on the rear end of the reactor, coaxially positioned with the reactor. The carbon black was discharged through the same opening at the end of the pyrolysis process. The steam-gas mixture exiting the reactor was directed to the condensation unit where it was divided into three liquid fractions differing by boiling point and named further conditionally light, medium and heavy, and gas fraction that was directed to the reactor heating and its surplus was utilized. The mass of material fed into the reactor averaged 6,120 kg, and the fraction of cargo tyres averaged 88%. At the output of the process, the proportion of liquid fuel was on average 35%, the proportion of carbon black was 29%, the proportion of metal waste was 21%, and the proportion of the gaseous fraction was 15%.

We studied the liquid fractions in order to compare their chemical composition with a sample of liquid heating oil produced by OAO "YaNPZ named after D.I. Mendeleev" (Mendeleev Oil Refinery), Yaroslavl region, Russia. The sample was produced according to TU 38.101656-99 from distillate fractions produced by direct distillation of oil and secondary processes of oil refining.

For the analysis we took samples of three pyrolysis fractions; only light and middle fractions are used as fuel; the heavy fraction is supposed to be used as plasticizer – softener for the rubber blends production. The density at 20 °C of the light fraction was on the average 835 kg/m<sup>3</sup>, the density of the medium fraction varied in the range 850-950 kg/m<sup>3</sup> depending on process conditions and tyre waste batch.

In this study we investigate the physical and chemical properties of the fuel by IR and UV spectroscopy as well as by high performance liquid chromatography (HPLC). IR spectra were obtained using an IR-Fourier RX-1 device; samples were prepared as a micro-layer between KRS5 glasses. UV spectra were taken on a Specord M40 device. Spectra were recorded in the cuvette  $d = 10$  mm. Liquid chromatography analyses were conducted using UV-VIS LCD 2563, detector UV -  $\lambda = 210, 254$  nm. Conditions for recording spectra: column C-18, 5  $\mu\text{m}$ , length 150 mm,  $d = 5$  mm, mobile phase acetonitrile – water (70-30), the speed of the mobile phase 0.6 ml/min. In order to assess the useability of the fuel, the combustion character using a liquid fuel nozzle burner according to GOST 27824-2000 was investigated.

In order to analyze the most probable reactions during elastomer pyrolysis, we conduct the quantum-chemical calculations of thermodynamic function changes in the corresponding reactions. The calculations were done by the density functional method [21, 22] with the hybrid exchange-correlation functional Becke, Lee, Yang & Parr [23] at DFT B3LYP/6-311G\*\* level of theory. The calculations were made using the ORCA software package [24].

The geometry of the molecular models was optimised during the calculations. We searched for the conformations with the minimum energy using the quasi-Newtonian BFGS (Broyden-Fletcher-Goldfarb-Shanno) method [25-28]. Also we optimized in the internal



coordinate system of the molecule in Z-matrix format. The criterion for the search completion was reaching the RMS Gradient of the total electronic energy of the molecular system to 0.00001 atomic units (Eh/bohr). Since the gradient search is not sufficient to find an extremum, the optimization was performed from several different starting conformations of the molecule. In addition, when calculating the thermodynamic functions, the presence of an extremum was checked on the basis of the vibrational analysis [29] – by the absence of negative natural values of the Hesse matrix at the point of the assumed extremum. The thermodynamic functions (enthalpy and Gibbs free energy) in the minimal energy conformation were calculated as the sum of the total DFT electron energy using the above described approximation and the thermodynamic component in the rigid rotator-harmonic oscillator approach at the standard reaction temperature calculated on the basis of vibrational analysis at the ideal gas state. The free energies of the reactions were calculated as the differences of the corresponding values for the reaction products and reagents under standard conditions. This methodology was previously used in [30], and there was achieved good agreement with experimental data.

## Results and discussion

Tables 1-3 show the results of the IR absorption spectra of the samples under study.

**Table 1.** Comparative analysis of IR spectra of a liquid fuel sample of the medium pyrolysis fraction and a fuel sample produced by OAO "YaNPZ named after D.I. Mendeleev"

Parameters	Rubber pyrolysis, medium fractions	OAO "YaNPZ named after D.I. Mendeleev"
Nature of the sample	Dark-coloured sample with a pungent smell	A sample of light yellow colour faintly smelling
Type of vibration	Vibrational frequencies in the IR spectrum, $\text{cm}^{-1}$	
Stretching vibrations ( $\nu$ ) -CH <sub>2</sub> -, -CH <sub>3</sub>	2955, 2924, 2854, 2868	2946, 2924, 2855, 2867
Bending ( $\delta$ ) -CH <sub>2</sub> -	1460	1456
Rocking vibrations (-CH <sub>2</sub> -) <sub>n</sub> ≥ 4 (-CH <sub>2</sub> -) <sub>n</sub> ≤ 4	722 756–746	722 740
Bending ( $\delta$ ) -CH <sub>3</sub>	1376	1377
Carbonyl-containing C=O groups	1706	-
Olefinic functionality C = C - <i>trans</i> -position -C=CH <sub>2</sub> - vinylidene	1658, 1641 966 886	- - -
Aromatics 1,4-substitution 1,2-substitution	1603, 1513, 1494 814 756	1607 possibly polyenes
Aromatics content, % Paraffin hydrocarbon content, % $\nu = 2855 \text{ cm}^{-1}$	6.6 11.54	~0.1 46.35


**Table 2.** Analysis of IR spectra of a liquid fuel sample of the light pyrolysis fraction

Parameters	Rubber pyrolysis, light fractions
Nature of the sample	A sample of light yellow colour smelling
Type of vibration	Vibrational frequencies in the IR spectrum, $\text{cm}^{-1}$
Stretching vibrations ( $\nu$ ) -CH <sub>2</sub> -, -CH <sub>3</sub>	2955, 2925, 2857, 2869
Bending ( $\delta$ ) -CH <sub>2</sub> -	1455
Rocking vibrations (-CH <sub>2</sub> -) <sub>n</sub> ≥ 4 (-CH <sub>2</sub> -) <sub>n</sub> ≤ 4	728 756, 743
Bending ( $\delta$ ) -CH <sub>3</sub>	1376
Carbonyl-containing C=O groups	1748, 1720
Olefinic functionality	1643
C = C - <i>trans</i> -position	966
-C=CH <sub>2</sub> - vinylidene	887
-HC=CH <sub>2</sub>	909, 990
Aromatics	1602, 1516, 1494
1,4-substitution	814
1,2-substitution	756
monosubstitution	756, 695
Aromatics content, %	15.15
Paraffin hydrocarbon content, % $\nu = 2857 \text{ cm}^{-1}$	12.6

**Table 3.** Analysis of IR spectra of a liquid fuel sample of the heavy pyrolysis fraction

Parameters	Rubber pyrolysis, heavy fractions
Nature of the sample	Dark-coloured sample with a pungent smell
Type of vibration	Vibrational frequencies in the IR spectrum, $\text{cm}^{-1}$
Stretching vibrations ( $\nu$ ) -CH <sub>2</sub> -, -CH <sub>3</sub>	2953, 2924, 2854, 2867
Bending ( $\delta$ ) -CH <sub>2</sub> -	1457
Rocking vibrations (-CH <sub>2</sub> -) <sub>n</sub> ≥ 4 (-CH <sub>2</sub> -) <sub>n</sub> ≤ 4	723 753
Bending ( $\delta$ ) -CH <sub>3</sub>	1376
Carbonyl groups C=O	1717, 1704
Olefinic functionality	1607(polyene)
C = C - <i>trans</i> -position	965
Aromatics	1601, 1514, 1496
1,4-substitution	813
1,2-substitution	753
Aromatics content, %	15.1
Paraffin hydrocarbon content, % $\nu = 2855 \text{ cm}^{-1}$	29.1



According to the results of IR spectra analysis it can be concluded that the fuel sample of OAO "YaNPZ named after D.I. Mendeleev" consists mainly of paraffin fractions, while pyrolysis fuel has a more complex chemical composition and in addition to paraffin hydrocarbons also includes aromatic hydrocarbons, unsaturated hydrocarbons, and a number of oxygen (carbonyl) containing compounds. The content of carbonyl compounds is relatively low. Also it is more noticeable on the light fraction of pyrolysis products and to a lesser extent on the medium and heavy ones. The relative content of paraffin hydrocarbons for pyrolysis products is the highest for the heavier fraction and the lowest for the medium fraction. The light fraction has approximately the same content of aromatic and paraffin hydrocarbons.

Analysis of the UV spectra of the pyrolysis rubber samples allowed the following observations to be made:

1) the light fraction has weak absorptions at  $\lambda_1 = 255.7$  nm (corresponding to aromatic and naphthenic hydrocarbons) and a lever in the range 217-244 nm (corresponding to coupled multiples and monosubstituted aromatic compounds with a long hydrocarbon radical). In addition, there is an intense absorption at  $\lambda_1 = 200-210$  nm, which corresponds to monosubstitution in the aromatic ring. The absorption at this range is covered by the solvent.

2) the medium fraction has intense absorptions at  $\lambda_1 = 257.7$  nm (corresponding to aromatic and naphthenic hydrocarbons) and a lever in the range 215-244 nm (corresponding to coupled multiples and monosubstituted aromatic compounds with a long hydrocarbon radical).

3) the heavy fraction has weak absorptions at  $\lambda_1 = 259.7$  nm (corresponding to aromatic and naphthenic hydrocarbons) and a lever in the range 213-244 nm (corresponding to coupled multiples and monosubstituted aromatic compounds with a long hydrocarbon radical).

The fuel sample of OAO "YaNPZ named after D.I. Mendeleev" has intense absorption at  $\lambda_1 = 224$  nm (which corresponds to coupled multiples), absorption at  $\lambda_2 = 255$  nm -- has a weakly marked nature.

The HPLC spectra of the light and medium fractions of the pyrolysis fuel are shown on Figures 1 and 2.

In according to the HPLC analysis it can be concluded that all the samples are characterised by a complex composition. The pyrolysis rubber samples contain light and heavy aromatic (for the light fraction mainly monosubstituted), and naphthenic components.

On the base of the analysis we can conclude that the investigated pyrolysis fuel is generally consistent in composition with the fuel compositions published in [16, 17], but characterised by a lower content of aromatic hydrocarbons.

The combustion character using a liquid fuel nozzle burner was assessed for samples of light and medium fraction of pyrolysis products and a fuel sample of OAO "YaNPZ named after D.I. Mendeleev". All three examined samples were characterized by a steady burning character. The most intense combustion was characterized by the sample of light fraction of the pyrolysis product; its flame colour was bluish, but the flame colour of the other two samples was red-orange. The temperature of the burner diffuser at the flame zone measured by pyrometer was 440 °C for the light fraction, 350 °C for the medium pyrolysis fraction and 340 °C for the OAO "YaNPZ named after D.I. Mendeleev" fuel sample, respectively.

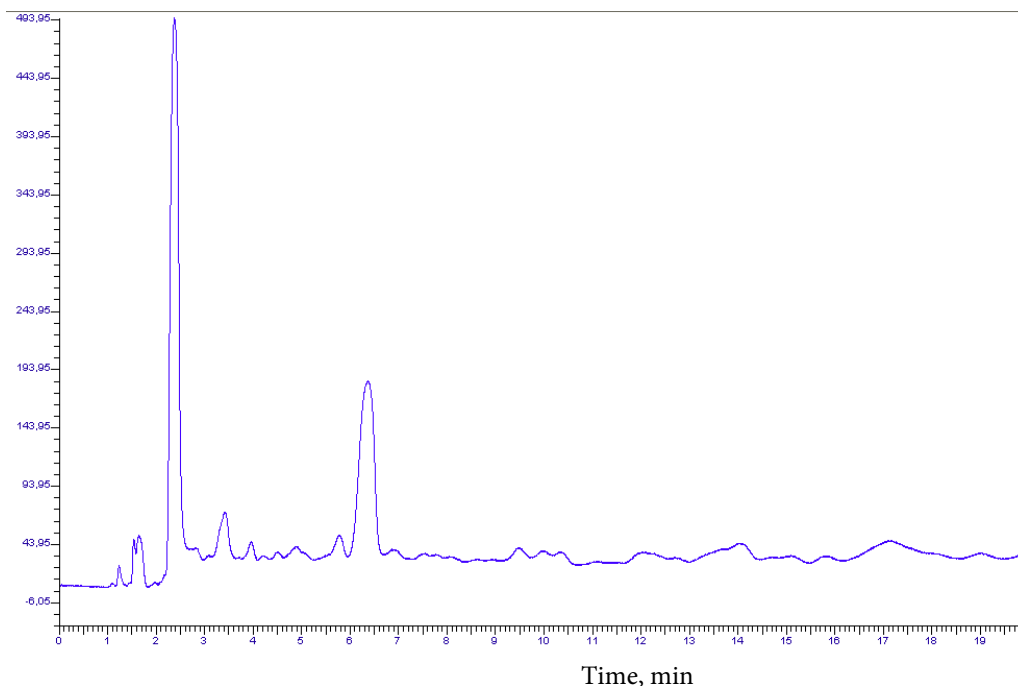


Fig. 1. The HPLC spectra of the light fraction of the pyrolysis fuel

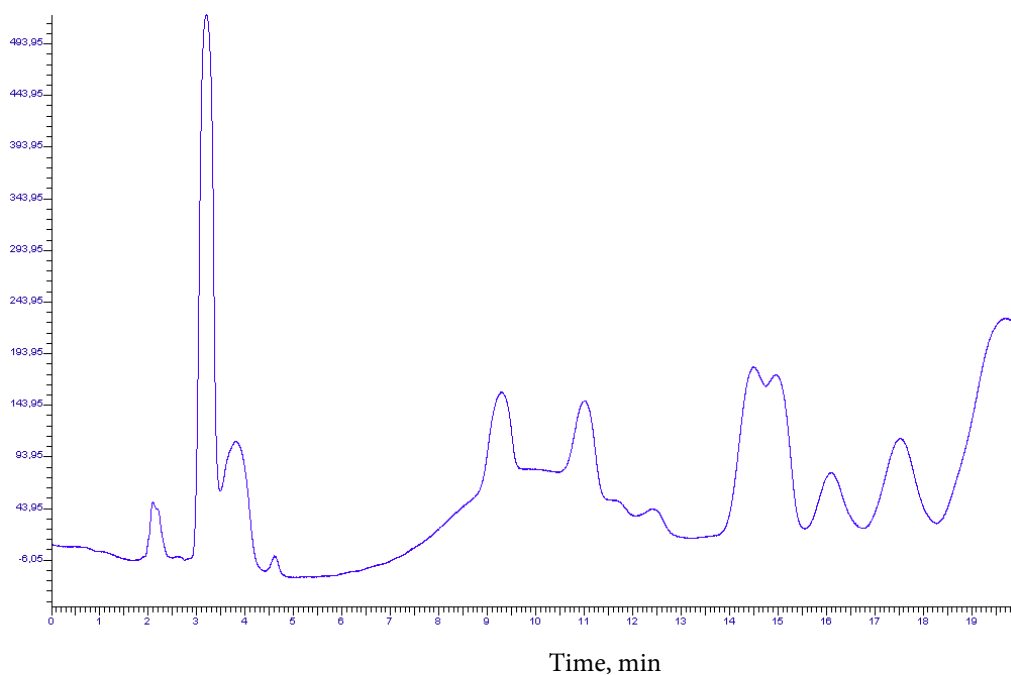


Fig. 2. The HPLC spectra of the medium fraction of the pyrolysis fuel

To summarize the study, we can conclude that despite the different chemical composition of pyrolysis fuel compared to batch petroleum fuel, it is not inferior to it in terms of consumer properties and even superior, if we consider the light fraction of pyrolysis.

As shown above, the pyrolysis process of waste rubber produces a large variety of chemical compounds as a result of the reactions involved. However, for modeling purposes, a formal scheme, within the framework of which a system of kinetic equations suitable for solving practical problems could be formulated, is sufficient. To substantiate such a scheme, quantum-chemical calculations of changes in thermodynamic functions in degradation reactions according to the radical-chain mechanism of compounds representing low-molecular-weight models of





elastomers included in tire rubbers were performed. Chemical formulas of the compounds and radical intermediates under study, their abbreviations and explanations are presented in Table 4. Tyre rubbers are made from three types of general purpose rubber: isoprene (natural and synthetic), butadiene, and butadiene-(methyl)styrene. The proportion of rubber varies according to the tyre type and manufacturer; isoprene rubber has the largest proportion, while butadiene rubber and butadiene styrene (methylstyrene) account for less than 40% in total. The low-molecular-weight models of these rubbers are designated as I-I, B-B, and mSt-B, respectively. As these rubbers are vulcanised with sulphur curing systems; the compound designated B-S-S-B was considered as a sulphur crossbond model. Radicals B<sup>·</sup>-B, I<sup>·</sup>-I, mSt-B modelled intermediates formed by hydrogen atom detachment at the  $\alpha$ -carbon atom of the respective bonds; I, B, mSt modelled intermediates formed by chain breakage, and B-S modelled intermediates formed by sulphur crossbond breakage. Compounds I, B, Bd modelled destruction reaction products.

**Table 4.** Chemical formulas and symbols of molecular models of rubbers, radical intermediates, and pyrolysis reaction products used in quantum-chemical simulations

Chemical formula	Symbol	Commentary
$\text{CH}_3\text{-CH=CH-CH}_2\text{-CH}_2\text{-CH=CH-CH}_3$	B-B	Double chain bond model of polybutadiene
$\text{CH}_3\text{-CH}^{\cdot}\text{-CH=CH-CH}_2\text{-CH=CH-CH}_3$	B <sup>·</sup> -B	Radical formed by hydrogen stripping at the $\alpha$ -carbon atom of a butadiene link
$\text{CH}_3\text{-CH=CH-CH}_3$	B	Butene-2, formed by detachment of the polybutadiene end-link
$\text{CH}_2\text{=CH-CH}^{\cdot}\text{-CH}_3$	B <sup>·</sup>	The butene radical formed by the detachment of the link
$\text{CH}_2\text{=C=CH-CH}_3$	Bd	Diene formed by a kinetic chain break
$\text{CH}_3\text{-CH=C(CH}_3\text{)-CH}_2\text{-CH}_2\text{-C(CH}_3\text{)=CH-CH}_3$	I-I	Double chain bond model of polyisoprene
$\text{CH}_3\text{-CH}^{\cdot}\text{-C(CH}_3\text{)=CH-CH}_2\text{-CH=CH-CH}_3$	I <sup>·</sup> -I	Radical formed by hydrogen stripping at the $\alpha$ -carbon atom of isoprene link
$\text{CH}_3\text{-C(CH}_3\text{)=CH-CH}_3$	I	2-methyl-butene-2, formed by detachment of the polyisoprene end link
$\text{CH}_2\text{=C(CH}_3\text{)-CH}^{\cdot}\text{-CH}_3$	I <sup>·</sup>	2-methyl-butene-2 radical, formed by detachment of the link
$\text{CH}_3\text{-CH=CH-CH}_2\text{-S-S-CH}_2\text{-CH=CH-CH}_3$	B-S-S-B	Sulphur cross-bonding model
$\text{CH}_3\text{-CH=CH-CH}_2\text{-S}^{\cdot}$	B-S <sup>·</sup>	Radical formed by sulphur cross-bonding breakage
$\text{CH}_3\text{-C(CH}_3\text{)(C}_6\text{H}_5\text{)-CH}_2\text{-CH}_2\text{-CH=CH-CH}_3$	mSt-B	Butadiene methylstyrene copolymer model
$\text{CH}_3\text{-C(CH}_3\text{)(C}_6\text{H}_5\text{)-CH}_2\text{-CH}^{\cdot}\text{-CH=CH-CH}_3$	mSt-B <sup>·</sup>	Radical butadiene styrene copolymer
$\text{CH}_3\text{-C(CH}_3\text{)(C}_6\text{H}_5\text{)-CH}_2^{\cdot}$	mSt <sup>·</sup>	Methylstyrene radical

Table 5 shows the results of quantum-chemical calculation of the total electron energy changes ( $\Delta E$ ) and free energy under standard conditions ( $\Delta G$ ) during radical-chain degradation



reactions of elastomers. Including: initiation by chain-breaking (1)-(3), transverse bonding (4); initiation by hydrogen stripping at  $\alpha$ -carbon atom (5)-(7); chain transfer to polymer (8), (9); linear chain-breaking with hydrogen formation (10); quadratic chain-breaking by disproportionation reaction (11).

**Table 5.** Changes of total electron energy and Gibbs free energy under standard conditions during radical-chain degradation reactions of elastomers by quantum-chemical calculations at the DFT B3LYP/6-311G\*\* level of theory

Number	Reaction scheme	$\Delta E, \text{kJ/mol}$	$\Delta G, \text{kJ/mol}$
1	$\text{B-B} \rightarrow 2\text{B}^\cdot$	439.2	142.1
2	$\text{I-I} \rightarrow 2\text{I}^\cdot$	422.8	141.9
3	$\text{mSt-B} \rightarrow \text{mSt}^\cdot + \text{B}^\cdot$	440.1	199.4
4	$\text{B-S-S-B} \rightarrow 2\text{B-S}^\cdot$	222.8	357.4
5	$\text{B-B} \rightarrow \text{B}^\cdot\text{-B} + \text{H}$	435.3	300.9
6	$\text{I-I} \rightarrow \text{I}^\cdot\text{-I} + \text{H}$	343.9	307.9
7	$\text{mSt-B} \rightarrow \text{mSt-B}^\cdot + \text{H}$	356.8	297.9
8	$\text{B-B} + \text{B}^\cdot \rightarrow \text{B}^\cdot\text{-B} + \text{B}$	-48.9	-16.6
9	$\text{I-I} + \text{I}^\cdot \rightarrow \text{I}^\cdot\text{-I} + \text{I}$	-146.9	-13.0
10	$\text{B}^\cdot \rightarrow \text{Bd} + 1/2\text{H}_2$	79.1	13.0
11	$2\text{B}^\cdot \rightarrow \text{Bd} + \text{B}$	-176.3	-98.8

Based on the results of quantum-chemical calculations, we can conclude that the main initiation mechanism during pyrolysis is the breaking of the polyisoprene and polybutadiene chains. The butadiene-methylstyrene copolymer units will be broken at a slower rate, since they require more energy. This is consistent with the known fact that butadiene styrene copolymers are more heat resistant. Hydrogen detachment initiation is less likely, as it requires more energy. As for the breakage of sulphur cross-links, although they are less strong than carbon-carbon ones, the formation of sulphide radicals is accompanied by a greater increase of free energy compared to other types of initiation. Therefore, for practical calculations, the initiation of chain degradation by the breaking of sulfide bonds can be disregarded. These bonds are rapidly broken, but in general the course of the radical-chain mechanism should not have a significant influence. Chain transfer reactions on the polymer (8), (9) are characterized by negative values  $\Delta E$  and  $\Delta G$  will provide the growth of kinetic chain degradation. By the comparison of changes in thermodynamic functions in reactions (10), (11) it can be concluded that the main chain breakage mechanism will be the quadratic chain breakage.

The kinetics of polymer thermal degradation is usually described using differential equations as follows:

$$\frac{d\alpha_i}{dt} = (1 - \alpha_i)^{n_i} A_i \exp(-E_i/RT), \quad (1)$$

where  $\alpha_i$  is the degree of conversion of the  $i$ -th reaction;  $n_i$  are the orders of reactions;  $A_i$  and  $E_i$  are the parameters of the Arrhenius equation of temperature dependences of reaction rate constants.



The disadvantage of this approach is the lack of connection of these empirical dependences with the mechanism of thermodestruction process. This leads to the fact that the parameters obtained by approximating the experimental thermogravimetric curves in different authors differ greatly, and sometimes do not correspond to the physical meaning of the kinetic equation of the reaction at all. Thus, in particular, the authors of [31] analyzed the data of eleven papers. These papers gave assessment of kinetic parameters of rubbers thermodegradation based on polybutadiene, butadiene-styrene copolymer, as well as worn tyres. The values of the reactions orders varied from 1 to 2 in the approximation dependences, and the values of activation energies  $E_i$  of different authors varied in the range of 60-600 kJ/mol. For the same polymer, at different heating rates, the kinetic parameters of the simple equations turn out to be different. It does not allow such schemes to be used when modelling real production reactors.

In the present study, a formal kinetic scheme was used to describe the kinetics of rubber degradation. It shows the general physical meaning of the process as a set of radical-chain reactions of polymer degradation. The proposed scheme presented by Table 6.

**Table 6.** Formal scheme of degradation reaction kinetics of polymer parts of worn tyres

Stage number	Reaction scheme	Commentary
1	$R-R \rightarrow 2R\cdot$	Initiation, $k_{0i}$
2	$R-R + R\cdot \rightarrow R\cdot-R + R$	Chain transfer to the polymer, $k_{1i}$
3	$R\cdot-R \rightarrow R\cdot + R$	Isomerisation of the middle radical with chain breaking, $k_{2i}$
4	$2R\cdot \rightarrow 2R$	Quadratic chain breaking by disproportionality, $k_{3i}$

Stage (1) represents all initiation reactions (1)-(4) shown in Table 5. Stage (2) refers to chain transfer reactions to polymer like (8), (9) in Table 5 and stage (3) symbolizes isomerization of formed radicals by disproportionation with chain breaking. Stage (4) symbolizes a quadratic break of kinetic chains by disproportionation reaction like (11) in Table 5.

R-R in this scheme means any polymer chain and R means any nonradical product of its decomposition. Thus, all types of monomer links and types of low molecular weight products resulting from chain decomposition are averaged. Since in the production process the vapour-gas mixture is separated into three fractions – gas, light and medium (the heavy fraction is not used and is returned to the recycle), three schemes corresponding to the three groups of compounds are provided to describe the whole destruction process. Each group has its own set of rate constants:  $k_{0i}, k_{1i}, k_{2i}, k_{3i}, i = 1, 2, 3$ . The temperature dependences of the rate constants were taken as Arrhenius dependences. Thus, the total three pairs of parameters were needed to identify one thermogravimetric curve  $A_i$  and  $E_i$  for each rate constant. The kinetics of the reactions corresponding to the three kinetic schemes are described by a set of three systems of differential equations:

$$\frac{dRR}{dt} = -k_{0i} * RR - k_{1i} * RR * Ra; \quad (2)$$

$$\frac{dRaR}{dt} = k_{1i} * RR * Ra - k_{2i} * RaR; \quad (3)$$



$$\frac{dRa}{dt} = 2k_{0i} * RR - k_{1i} * RR * Ra + k_{2i} * RaR - 2k_{3i} * Ra * Ra; \quad (4)$$

$$\frac{dR}{dt} = k_{1i} * RR * Ra + k_{2i} * RaR + 2k_{3i} * Ra * Ra. \quad (5)$$

To avoid confusion R-R is denoted here as RR; R' is denoted as Ra; R'-R is denoted as RaR and the symbol "\*" is used as the multiplication sign.

At a time-varying temperature, the reaction rate constants according to the Arrhenius equations also become functions of time. The systems of equations (2)-(5) for  $i = 1, 2, 3$  were integrated numerically with respect to the given temperature-time dependences. The total time dependence of degradable polymer mass in relative units  $Y(t)$  was described as a weighted sum of functions  $RR_i(t)$  of three groups of compounds:

$$Y(t) = \sum_i b_i RR_i(t), \quad (6)$$

where  $b_i$  is the relative proportion of each group ( $\sum_i b_i = 1$ ).

This approach makes it possible to approximate the thermal degradation curves of rubbers based on general-purpose rubbers. As an example, Fig. 3 shows experimental data on thermo-destruction of rubbers, published by different authors, and approximated by their functions, according to the outlined methodology.

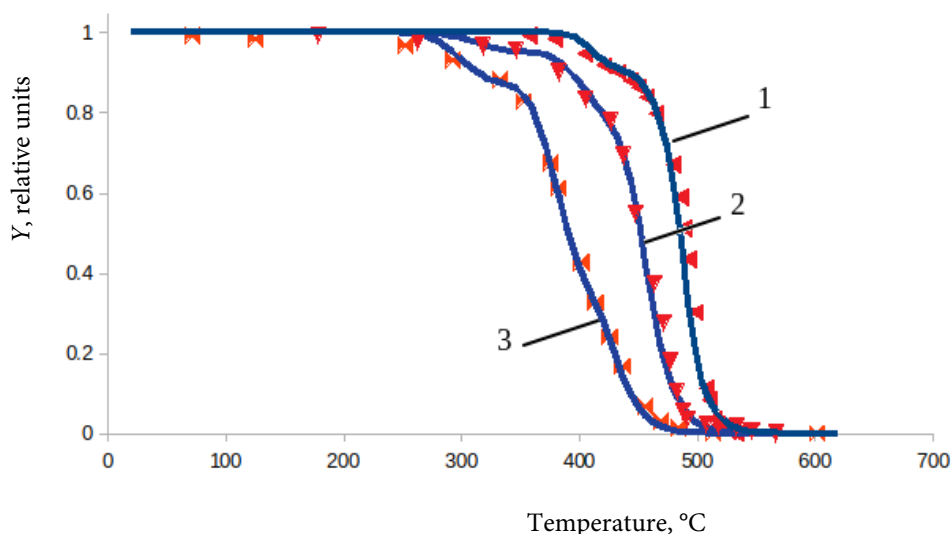


**Fig. 3.** Dependence of the relative polymer mass fraction on temperature according to thermogravimetric analysis and approximation curves (solid) according to the proposed mathematical model. Dots - experiment: 1 - according to experimental data [32]: 1,4-*cis*-polybutadiene, heating rate  $dT/dt = 10$  K/min; 2 - from experimental data [31]: polybutadiene,  $dT/dt = 5$  K/min; 3 - from experimental data [18]: rubber from worn tyres,  $dT/dt = 15$  K/min. Experimental data standardised to the initial polymer mass

The proposed mathematical model of degradation kinetics can be seen to describe thermogravimetric curves relating to different types of rubbers and different heating rates. This makes it possible to use the proposed approach to construct a mathematical model of the production reactor in the form of a coupled problem of non-stationary thermal conductivity and chemical kinetics.



## Conclusions and recommendations

This paper presents a formal kinetic scheme and corresponding model of rubber thermo-degradation process during pyrolysis of used automobile tyres and rubber waste in an industrial reactor. Parameters of the model were made on the basis of the analysis of pyrolysis products of the worn tyres on the real industrial reactor. Also we used the quantum-chemical calculations of the reaction thermodynamics for the compounds simulating the structure of the polymeric part of the waste material. The reaction products under study are the solid fraction (carbon black and metal wastes), and the vapour-gas mixture separated into three hydrocarbon fractions. The proposed formal kinetic scheme shows the general physical meaning of the process as a set of radical-chain reactions of polymer degradation. We used the individual set of kinetic constants for each hydrocarbon fraction. The temperature dependences of the constants are assumed to be Arrhenius. This approach makes it possible to approximate the thermodestruction curves of rubbers based on general-purpose rubbers. It is confirmed by comparing the calculated thermogravimetric curves with the experimental data published by different authors for different types of rubber waste. The proposed approach can be used in modelling and optimising the operation of an industrial rubber waste pyrolysis reactor by solving the coupled problem of unsteady thermal conductivity and chemical kinetics.

## References

1. **Bandyopadhyay, S., Agrawal, S.L., Ameta, R., Dasgupta, S., Mukhopadhyay, R., Deuri, A.S. & Suresh, C.** (2008) An Overview of Rubber Recycling, *Progress in Rubber, Plastics and Recycling Technology*, 24(2), pp. 73-112 [online]. Available at: <https://doi.org/10.1177/147776060802400201>
2. **Sienkiewicz, M., Kucinska-Lipka, J., Janik, H. & Balas, A.** (2012) Progress in used tyres management in the European Union: A review, *Waste Management*, 32(10), pp. 1742-1751 [online]. Available at: <https://doi.org/10.1016/j.wasman.2012.05.010>
3. **Myhre, M., Saiwari, S., Dierkes, W. & Noordermeer, J.** (2012) Rubber recycling: chemistry, processing, and applications, *Rubber Chemistry and Technology*, 85(3), pp. 408-449 [online]. Available at: <https://doi.org/10.5254/rct.12.87973>
4. **Roy, C., Chaala, A. & Darmstadt, H.** (1999) The vacuum pyrolysis of used tires: End-uses for oil and carbon black products, *Journal of Analytical and Applied Pyrolysis*, 51(1-2), pp. 201-221 [online]. Available at: [https://doi.org/10.1016/S0165-2370\(99\)00017-0](https://doi.org/10.1016/S0165-2370(99)00017-0)
5. **Kaminsky, W., Mennerich, C. & Zhang, Z.** (2009) Feedstock recycling of synthetic and natural rubber by pyrolysis in a fluidized bed, *Journal of Analytical and Applied Pyrolysis*, 85(1-2), pp. 334-337 [online]. Available at: <https://doi.org/10.1016/j.jaap.2008.11.012>
6. **Czajczyńska, D., Czajka, K., Krzyżyńska & R., Jouhara, H.** (2020) Waste tyre pyrolysis – Impact of the process and its products on the environment, *Thermal Science and Engineering Progress*, 20, 100690 [online]. Available at: <https://doi.org/10.1016/j.tsep.2020.100690>
7. **Khalil, U., Vongsvivut, J., Shahabuddin, M., Samudrala, S.P., Srivatsa, S.C. & Bhattacharya, S.** (2020) A study on the performance of coke resistive cerium modified zeolite Y catalyst for the pyrolysis of scrap tyres in a two-stage fixed bed reactor, *Waste Management*, 102, pp. 139-148 [online]. Available at: <https://doi.org/10.1016/j.wasman.2019.10.029>
8. **Hijazi, A., Al-Muhtaseb, A.H., Aouad, S., Ahmad, M.N. & Zeaiter, J.** (2019) Pyrolysis of Waste Rubber Tires with Palladium Doped Zeolite, *Journal of Environmental Chemical Engineering*, 7(6), 103451 [online]. Available at: <https://doi.org/10.1016/j.jece.2019.103451>



9. Wang, F., Gao, N., Quan, C. & López, G. (2019) Investigation of Hot Char Catalytic Role in the Pyrolysis of Waste Tires in a Two-step Process, *Journal of Analytical and Applied Pyrolysis*, 146, 104770 [online]. Available at: <https://doi.org/10.1016/j.jaap.2019.104770>
10. Islam, M.R., Parveen, M., Haniu, H. & Sarker, M.R.I. (2010) Innovation in Pyrolysis Technology for Management of Scrap Tire: a Solution of Energy and Environment, *International Journal of Environmental Science and Development*, 1(1), pp. 89-96. DOI: 10.7763/IJESD.2010.V1.18.
11. Yaqoob, H., Teoh, Y.H., Ahmad, M. & Gulzar, M. (2021) Potential of tire pyrolysis oil as an alternate fuel for diesel engines: A review, *Journal of the Energy Institute*, 96, pp. 205-221 [online]. Available at: <https://doi.org/10.1016/j.joei.2021.03.002>
12. Mikulski, M., Ambrosewicz-Walacik, M., Hunicz, J. & Nitkiewicz, S. (2021) Combustion engine applications of waste tyre pyrolytic oil, *Progress in Energy and Combustion Science*, 85, 100915 [online]. Available at: <https://doi.org/10.1016/j.pecs.2021.100915>
13. Yaqoob, H., Teoh, Y.H., Sher, F., Jamil, M.A., Nuhanović, M., Razmkhah, O. & Erten, B. (2021) Tribological Behaviour and Lubricating Mechanism of Tire Pyrolysis Oil, *Coatings*, 11, 386, pp. 1-13 [online]. Available at: <https://doi.org/10.3390/coatings11040386>
14. Kyari, M., Cunliffe, A. & Williams, P.T. (2005) Characterization of Oils, Gases, and Char in Relation to the Pyrolysis of Different Brands of Scrap Automotive Tires, *Energy & Fuels*, 19, pp. 1165-1173. URL: <https://doi.org/10.1021/ef049686x>
15. Pavlova, A., Stratiev, D., Mitkova, M., Stanulov, K., Dishovsky, N. & Georgiev, K. (2015) Gas Chromatography-Mass Spectrometry for Characterization of Liquid Products from Pyrolysis of Municipal Waste and Spent Tyres, *Acta Chromatographica*, 1, pp. 1-19 [online]. Available at: <https://doi.org/10.1556/achrom.27.2015.4.5>
16. Campuzano, F., Jameel, A.G.A, Zhang, W., Emwas, A.-H., Agudelo, A.F., Martínez, J.D. & Mani Sarathy, S.M. (2020) Fuel and Chemical Properties of Waste Tire Pyrolysis Oil Derived from a Continuous Twin-Auger Reactor, *Energy & Fuels*, 34(10), pp. 12688–12702 [online]. Available at: <https://doi.org/10.1021/acs.energyfuels.0c02271>
17. Abedeen, A., Hossain, M.S., Som, U. & Moniruzzaman, M.D. (2021) Catalytic cracking of scrap tire-generated fuel oil from pyrolysis of waste tires with zeolite ZSM-5, *International journal of sustainable engineering*, 14(6), pp. 2025-2040 [online]. Available at: <https://doi.org/10.1080/19397038.2021.1951883>
18. Mkhize, N.M., Danon, B., van der Gryp, P. & Görgens, J.F. (2019) Kinetic study of the effect of the heating rate on the waste tyre pyrolysis to maximise limonene production, *Chemical Engineering Research and Design*, 152, pp. 363–371 [online]. Available at: <https://doi.org/10.1016/j.cherd.2019.09.036>
19. Nkosi, N., Muzenda, E., Mamvura, T.A., Belaid, M. & Patel, B. (2020) The Development of a Waste Tyre Pyrolysis Production Plant Business Model for the Gauteng Region, South Africa, *Processes*, 8(7), pp. 766-774 [online]. Available at: <https://doi.org/10.3390/pr8070766>
20. Rani, S. & Agnihotri, R. (2014) Recycling of scrap tyres, *International Journal of Materials Science and Applications*, 3(5), pp. 164-167 [online]. Available at: <https://doi.org/10.11648/j.ijmsa.20140305.16>
21. Hohenberg, P. & Kohn, W. (1964) Inhomogeneous Electron Gas, *Phys. Rev.*, 136, 3B, pp. B864-B871 [online]. Available at: <https://doi.org/10.1103/PhysRev.136.B864>
22. Kohn, W. & Sham, L.J. (1965) Self-Consistent Equations Including Exchange and Correlation Effects, *Phys. Rev.*, 140, 4A, pp. A1133-A1138 [online]. Available at: <https://doi.org/10.1103/PhysRev.140.A1133>
23. Becke, A.D. (1993) Densityfunctional thermochemistry. III. The role of exact exchange, *J. Chem. Phys.*, 98(7), pp. 5648–5652 [online]. Available at: <https://doi.org/10.1063/1.462066>
24. Neese, F. (2017) Software update: the ORCA program system, version 4.0, *Wiley Interdiscip. Rev.: Comput. Mol. Sci.*, 8, e1327 [online]. Available at: <https://doi.org/10.1002/wcms.1327>
25. Broyden, C.G. (1970) The convergence of a class of double-rank minimization algorithms, *Journal of Applied Mathematics*, 6, pp. 76–90 [online]. Available at: <https://doi:10.1093/imamat/6.1.76>
26. Fletcher, R.A. (1970) New Approach to Variable Metric Algorithms, *Computer Journal*, 13(3), pp. 317–322 [online]. Available at: <https://doi:10.1093/comjnl/13.3.317>
27. Goldfarb, D.A. (1970) Family of Variable-metric methods Updates Derived by Variational Means, *Mathematics of Computation*, 24(109), pp. 23–26 [online]. Available at: <https://doi:10.1090/S0025-5718-1970-0258249-6>



28. **Shanno, D.F.** (1970) Conditioning of quasi-Newton methods for function minimization, *Mathematics of Computation*, 24(111), pp. 647–656 [online]. Available at: <https://doi.org/10.1090/S0025-5718-1970-0274029-X>
29. **Mueller, M.** (2002) *Fundamentals of Quantum Chemistry. Molecular Spectroscopy and Modern Electronic Structure Computation*. New York (NY): Kluwer Academic publisher [online]. Available at: <https://doi.org/10.1063/1.1535013>
30. **Varvarkin, S.V., Soloviev, M.E. & Gerasimova, N.P.** (2022) Quantum-chemical study of the carboxylation reaction of 4-aminophenol, 4-acetylaminophenol and their salts in the synthesis of 5-aminosalicylic acid, *From Chemistry Towards Technology Step-By-Step*, 3(3), pp. 27-33. DOI: 10.52957/27821900\_2022\_03\_27 [online]. Available at: [https://drive.google.com/file/d/1k3uNF\\_opZcwn\\_-W9gFfgZ6o4PLJ3BBSf/view](https://drive.google.com/file/d/1k3uNF_opZcwn_-W9gFfgZ6o4PLJ3BBSf/view) (in Russian).
31. **Lin, J.-P., Chip Yuan, Chang, C., Wu, C.-H. & Shih, S.-M.** (1996) Thermal degradation kinetics of polybutadiene rubber, *Polymer Degradation and Stability*, 53, pp. 295-300 [online]. Available at: [https://doi.org/10.1016/0141-3910\(96\)00098-5](https://doi.org/10.1016/0141-3910(96)00098-5)
32. **McCree, K. & Keskkula, H.** (1979) Effect of thermal crosslinking on decomposition of polybutadiene, *Polymer*, 20, pp. 1155-1159 [online]. Available at: [https://doi.org/10.1016/0032-3861\(79\)90309-4](https://doi.org/10.1016/0032-3861(79)90309-4)

Received 12.01.2023

Approved after reviewing 17.03.2023

Accepted 22.03.2023